Modeling the mammalian locomotor CPG: insights from mistakes and perturbations

David A. McCrea[1,*] and **Ilya A. Rybak**[2]

1 *Spinal Cord Research Centre and Department of Physiology, University of Manitoba, Winnipeg, MB, R3E 3J7, Canada*

2 *Department of Neurobiology and Anatomy, Drexel University College of Medicine, Philadelphia, PA 19129, USA*

Abstract

A computational model of the mammalian spinal cord circuitry incorporating a two-level central pattern generator (CPG) with separate half-center rhythm generator (RG) and pattern formation (PF) networks is reviewed. The model consists of interacting populations of interneurons and motoneurons described in the Hodgkin-Huxley style. Locomotor rhythm generation is based on a combination of intrinsic (persistent sodium current dependent) properties of excitatory RG neurons and reciprocal inhibition between the two half-centers comprising the RG. The two-level architecture of the CPG was suggested from an analysis of deletions (spontaneous omissions of activity) and the effects of afferent stimulation on the locomotor pattern and rhythm observed during fictive locomotion in the cat. The RG controls the activity of the PF network that in turn defines the rhythmic pattern of motoneuron activity. The model produces realistic firing patterns of two antagonist motoneuron populations and generates locomotor oscillations encompassing the range of cycle periods and phase durations observed during cat locomotion. A number of features of the real CPG operation can be reproduced with separate RG and PF networks, which would be difficult if not impossible to demonstrate with a classical single-level CPG. The two-level architecture allows the CPG to maintain the phase of locomotor oscillations and cycle timing during deletions and during sensory stimulation. The model provides a basis for functional identification of spinal interneurons involved in generation and control of the locomotor pattern.

Keywords

spinal cord; CPG; rhythm generation; locomotion; afferent control

Introduction

Well co-ordinated locomotor activity can be evoked in the mammalian spinal cord in the absence of input from higher brain centers (e.g., in spinalized animals) and rhythmic sensory feedback following neuromuscular blockade, i.e., during fictive locomotion (see Grillner, 1981; Rossignol, 1996; Orlovsky et al., 1999). Such observations have provided evidence for the existence of a central pattern generator (CPG) that generates the locomotor rhythm and pattern of motoneuron activity (Graham Brown, 1914). There appears to be one CPG controlling each limb (see Yamaguchi, 2004; Zehr and Duysens, 2004) since there can be independent rates of left and right stepping in the legs of man (Dietz, 2003; Yang et al., 2004) and in spinal cats (e.g., Forssberg et al., 1980). Cats can also step with independent rates between the fore and hind limbs (Akay et al., 2006). The spinal cord also contains circuitry for

*Corresponding author. Tel.: +1 204 789 3770; Fax: +1 204 789 3930; E-mail: dave@scrc.umanitoba.ca.

inter-limb coordination, since coordinated stepping between the fore and the hind limbs is seen in animals with a spinal transection at upper cervical levels (Miller and van der Meche, 1976) and gaits remain matched and coordinated in the hind limbs of cats spinalized at mid-thoracic levels when walking on a treadmill (Forssberg et al., 1980).

The first conceptual scheme of the mammalian locomotor CPG responsible for alternating rhythmic extensor and flexor activity was based on a half-center concept (Graham Brown, 1914). According to the classical half-center architecture and its elaboration by Lundberg and colleagues (see Lundberg, 1981), the locomotor rhythm and the alternating activation of flexor and extensor motoneurons within a limb are produced by a single network consisting of two populations of excitatory interneurons (called the flexor and extensor half-centers) coupled together by reciprocal inhibitory connections such that activity in one half-center inhibits activity in the other. The interplay between tonic excitation of the two half-centers, a fatigue process reducing half-center activity over time, and the reciprocal inhibition between the half-centers results in rhythmic alternating activation of flexor and extensor motoneurons. The advantages of the half-center CPG organization include its relative simplicity and the strict alternation and coupling of flexor and extensor activities. This simple half-center architecture, however, is unable to account for a number of observations including the variety of motoneuron firing patterns observed during locomotion (e.g., Grillner, 1981; Stein and Smith, 1997).

The objective of the present study was to develop a computational model of the neural circuitry in the spinal cord that could provide predictions about the organization of the locomotor CPG and the interactions between the CPG and reflex circuits. We wished to create a model that could reproduce and provide explanations for a series of observations obtained in decerebrate adult cats during fictive locomotion induced by continuous electrical stimulation of the brainstem midbrain locomotor region (MLR) following neuromuscular blockade. One advantage of this preparation is that locomotor activity occurs without descending cortical influences, rhythmic sensory feedback, or the effects of systemic drug administration. Furthermore, the use of an adult preparation avoids developmental issues associated with an immature central and peripheral nervous system. Importantly, the pattern of motoneuron activities recorded in the decerebrate, immobilized cat during fictive locomotion is similar to that in intact preparations (Rossignol, 1996). Our intention was to develop a model in which a variety of simulations could be directly compared to data obtained during fictive locomotion in our laboratory. The simulations to be discussed were limited to creating locomotor-like activity in "pure" flexor and extensor motoneurons. The complex activity of motoneurons innervating muscles spanning more than one joint (bifunctional) is not considered here.

The role of intrinsic neuronal properties and reciprocal inhibition in rhythm generation

The major difficulty in developing a realistic CPG model is that the intrinsic and network mechanisms involved in the generation of the mammalian locomotor rhythm remain largely unknown. It is not yet possible to explicitly model the exact mechanisms operating in the mammalian spinal rhythm generator (RG). Therefore, our approach was to use the available data on spinal CPG operation and to incorporate rhythmogenic mechanisms operating in other mammalian CPGs and vertebrate motor systems. Our goal was to reproduce experimentally observed patterns of motoneuron activity recorded in the cat and their alteration under different conditions. At a minimum the model should be able to generate the locomotor rhythm and reproduce the following characteristics of fictive locomotion: (1) Tonic excitatory drive to the CPG (e.g., excitation mimicking that produced by tonic stimulation of the MLR) should evoke rhythmic activity with two alternating phases ("flexion" and "extension") coupled without intervening quiescent periods. (2) Increasing tonic (MLR) drive to the RG should result in a faster locomotor cadence. (3) Drive-evoked oscillations must encompass the range of step cycle

periods and flexor and extensor phase durations observed during fictive locomotion. (4) In the absence of MLR drive, an increase in the excitability of CPG neurons should produce slow locomotor-like activity similar to that evoked by systemic L-DOPA administration in cats. (5) Blocking synaptic inhibition should result in spontaneous synchronized oscillations of flexors and extensors.

There is indirect evidence for the involvement of the persistent (or slowly inactivating) sodium current, I_{NaP}, in rhythmogenesis in different motor systems. For example, this current was shown to play a critical role in respiratory rhythm generation in the pre-Bötzinger complex in vitro and under certain conditions, in vivo (Smith et al., 2000; Rybak et al., 2003, 2004; Paton et al., 2006). Persistent sodium currents have been found in spinal interneurons and motoneurons (e.g., Lee and Heckman, 2001; Darbon et al., 2004; Brocard et al., 2006; Dai and Jordan, 2006; Streit et al., 2006; Theiss et al., 2007), and its blockade (e.g., by riluzole) abolishes the intrinsic cellular oscillations and rhythm generation in cultured rat spinal cord neurons (Darbon et al., 2004; Streit et al., 2006) as well as the NMDA- and 5-HT-evoked fictive locomotor rhythm in the neonatal mouse spinal cord (Zhong et al., 2006). Based on this indirect evidence, we hypothesized that I_{NaP} plays an essential role in the generation of locomotor oscillations in the mammalian spinal cord and incorporated an I_{NaP}-dependent intrinsic oscillatory mechanism in our model of locomotor rhythm generation (Rybak et al., 2006a).

Figure 1A shows the schematic of the spinal locomotor RG implemented in our model. The RG contains a homogenous population of excitatory neurons with intrinsic I_{NaP}-dependent rhythmogenic properties. This homogenous population is subdivided into two half-centers (RG-E and RG-F populations) with excitatory synaptic connections within and between the half-centers. These half-centers reciprocally inhibit each other via corresponding inhibitory interneuron populations (Inrg-E and Inrg-F, see Fig. 1A). Each population in the model contains 20 neurons described as single-compartment, Hodgkin-Huxley type neuron models. Each neuron contains only a minimum set of ionic channels: fast sodium, potassium rectifier, and leakage channels. The excitatory RG and PF neurons also contain the persistent (slowlyinactivating) I_{NaP} sodium current. Because voltage- and time-dependent kinetics of activation and inactivation of fast sodium and potassium rectifier channels in mammalian spinal neurons have not been experimentally characterized, generic descriptions of these channels (from Booth et al., 1997) were used in the model. The kinetics of the NaP channel was adapted from previous computational models of neurons in the medullary pre-Bötzinger complex (Butera et al., 1999a, b; Rybak et al., 2003, 2004). The conductance of the NaP channel is characterized by a slow inactivation and is described as the product of three variables: the channel maximum conductance (g_{NaP}), the voltage- and time-dependent activation (m_{NaP}), and inactivation (h_{NaP}). The heterogeneity of neurons within each population was set by a random distribution of neuronal parameters and initial conditions. A full description of the model may be found in Rybak et al. (2006a).

Figure 1B illustrates the results of simulation of MLR-evoked locomotor rhythm in our model. The top three traces show, respectively: the histogram of average neuron activity in the RG-F population, the membrane potential trajectory of one neuron in this population, and the change in the inactivation variable for the NaP channel (h_{NaP}) in the same neuron. The next three traces show the same variables for the RG-E population. Locomotor oscillations in the model are initiated and maintained by a constant excitatory (MLR) drive to both RG populations. This drive is sufficient to depolarize the neurons of the excitatory populations to exceed the threshold for activation of the fast sodium current and to maintain spiking activity even if the persistent sodium current I_{NaP} becomes fully inactivated. In neurons of the currently active RG population, I_{NaP} progressively decreases with time because of the falling h_{NaP} (see third and sixth traces in Fig. 1B). The reduction in I_{NaP} reduces neuronal firing rate and population activity during the burst (see first and fourth traces), but activity remains sufficient to maintain

inhibition of the antagonist RG population via the corresponding Inrg population (Fig. 1B, two bottom traces).

At the same time, in neurons of the inhibited RG population (i.e., during the "off" phase of the locomotor cycle) I_{NaP} activation threshold progressively decreases (i.e., h_{NaP} increases). At some point I_{NaP} becomes activated and neuronal firing is initiated. Recurrent excitation within the half-center (see Fig. 1A) synchronizes the onset of firing in the population. The maximal activation of both the fast and the persistent sodium currents results in a high level of RG population activity with the onset of firing. This vigorous activity excites the corresponding Inrg population, which in turn inhibits the previously active (opposite) RG population. Repetition of these processes produces alternating bursts of firing in the RG-E and RG-F populations. In summary, the onset of firing bursts in our model is determined mostly by the activation of the intrinsic excitatory mechanism (I_{NaP}), whereas burst termination is determined by reciprocal inhibition. As a result, the cycle period (T) depends on the external (MLR) drive to RG half-centers, the reciprocal inhibition between them, and the intrinsic characteristics of NaP channels in RG neurons.

The effects of altering these parameters on cycle period (T) are shown in Figs. 1C1–C4. Consistent with the cat fictive locomotor preparation (Sirota and Shik, 1973), T decreases monotonically with increasing MLR drive (see Fig. 1C1). The increase in drive to each RG population in the model mainly affects the inter-burst interval (i.e., the currently silent RG population). Because of the drive-induced increase in excitability, h_{NaP} needs less time to reach the level at which the neuronal excitability overcomes the inhibition provided by the currently active (opposite) half-center. As a result phase switching occurs sooner and cycle period decreases. A decrease in T resulting from increased drive to both RG populations is illustrated in Fig. 1C1. Conversely, increasing the strength of reciprocal inhibition between the RG half-centers (mediated by the inhibitory Inrg populations) increases T. This is because more time is required for h_{NaP} to reach the level at which the neuronal excitability overcomes the increased inhibition (Fig. 1C2). Increasing the maximal conductance of NaP channels (g_{NaP}) in the RG neurons decreases T (Fig. 1C3) since the inactivation variable h_{NaP} needs less time during the inter-burst interval to reach the threshold and produce phase switching. Finally, increasing the maximal time constant for h_{NaP} increases T (Fig. 1C4) because h_{NaP} needs more time to reach the level of I_{NaP} activation during each inter-burst interval.

One important aspect for model evaluation is the ability to reproduce behaviors of the locomotor system observed in other experimental conditions. For this reason, we have used the model to simulate locomotor-like activity evoked without MLR stimulation by the application of monoamine neuromodulators or neuromodulators and to simulate rhythmic activity evoked by blocking spinal synaptic inhibition. We suggest that monoamine cause a net increase in neuron excitability. Such an increase could result, for example, from the 2 to 7 mV reduction in action potential threshold produced by both serotonin and nor-adrenaline in spinal cord in vitro preparations (Fedirchuk and Dai, 2004) or from a reduction of potassium leak conductance (e.g., Kjaerulff and Kiehn, 2001; Perrier et al., 2003). To imitate a pharmacologically induced increase in excitability in the model, the average leakage reversal potential E_L was depolarized in all RG neurons. Figure 2A shows that in the absence of MLR drive, a depolarization of E_L by 6 mV evoked slow locomotor-like oscillations with alternating flexor and extensor activities and $T \approx 5$ s. Although the lack of experimental data on neuromodulator mechanisms in the spinal cord precludes more detailed simulations, these oscillations in the model are qualitatively similar to the slower rhythms evoked by neuromodulators such as L-DOPA.

As described above, the inhibitory interneuron populations, Inrg-F and Inrg-E, are responsible for producing the strictly alternating activity between the half-centers. In our model these

populations have a low-level background activity, which prevents rhythm generation at rest. This low-level activity is also present between the strong bursts of activity evoked from the corresponding RG populations (bottom traces in Figs. 1B and 2A). As shown experimentally, antagonists of glycinergic and GABAergic inhibition can produce rhythmic activity characterized by synchronized bursting in flexor and extensor motoneurons (e.g., Noga et al., 1993;Cowley and Schmidt, 1995;Kremer and Lev-Tov, 1998;Beato and Nistri, 1999) instead of an alternating, locomotor pattern. To simulate oscillations evoked by blocking inhibitory transmission, the weights of all inhibitory connections in the model were set to zero. Under these conditions, the model generated oscillations in RG-F and RG-E that were synchronized by the excitatory connections between the two half-centers (see Fig. 2B) and are qualitatively similar to the synchronized activity evoked experimentally by blocking synaptic inhibition. Without reciprocal inhibition, cycle period is determined mainly by the level of neuronal excitability and the kinetics of I_{NaP} inactivation.

The finding that synchronized oscillations are evoked when synaptic inhibition is blocked in mammalian spinal cord preparations (Noga et al., 1993; Cowley and Schmidt, 1995; Kremer and Lev-Tov, 1998; Beato and Nistri, 1999) has led to the suggestion that the spinal locomotor network has endogenous rhythmogenic properties, which do not require inhibition (Kiehn, 2006; Rossignol et al., 2006). While we agree that a rhythm can be produced in the absence of network inhibition and our model can indeed produce such a rhythm, we do not accept that these oscillations represent the locomotor rhythm. Flexor and extensor bursts are strictly alternating during fictive locomotion, and this coupling is maintained as flexor and extensor phase durations are changed or interrupted by sensory stimulation. Alternating and strict coupling of flexor and extensor activities in a variety of preparations and throughout the entire range of locomotor speeds support the concept that reciprocal inhibition is essentially involved in at least the termination of flexor and extensor discharges and hence in locomotor-phase switching. For this reason, the locomotor pattern generated in our model is strongly dependent on the reciprocal inhibition between the RG half-centers (Fig. 1C2). We believe that regardless of the intrinsic rhythmogenic properties of spinal neurons involved, reciprocal inhibitory interactions are critically important for locomotor rhythm and pattern generation.

Much more needs to be learned about how and which intrinsic cellular mechanisms underlie mammalian locomotion. The locomotor rhythm in our model is generated with an essential contribution from the slowly inactivating sodium current (I_{NaP}). Our hypothesis originates from the role of this current in rhythmogenesis in other mammalian systems including respiratory rhythm generation and the presence of this current in mammalian spinal cord. Without further experimental evidence, it may be premature to claim that the I_{NaP}-dependent mechanism described in our model operates in the real spinal cord during locomotion. Mechanisms described in other preparations (see El Manira et al., 1994; Büschges et al., 2000; Grillner et al., 2001; Butt et al., 2002; Grillner and Wallén, 2002; Grillner, 2003) may also be important for rhythm generation. Our simulations do show, however, that I_{NaP}-dependent cellular properties of RG neurons in combination with reciprocal inhibition between the RG half-centers can reproduce locomotor oscillations as well as rhythmic activities evoked by neuromodulators and disinhibition (Fig. 2A and B).

Structure and operation of the locomotor model

The architecture of the locomotor model shown in Fig. 3A was suggested from two independent lines of experimental evidence obtained during fictive locomotion in cats. One series of experimental studies concerned deletions of motoneuron activity that occur during fictive locomotion in the cat. Deletions are brief periods during locomotion in which the normal alternating activity of flexor and extensor motoneurons is briefly interrupted by a failure to activate a group of synergist motoneurons. Because deletions occur spontaneously without any

experimental intervention and simultaneously affect multiple agonist motoneuron pools, it is likely that they result from spontaneous alterations in the excitability of some elements of the CPG and are not simply changes in the excitability of a few motoneurons. For example, the activity of all synergist motoneurons in the limb (e.g., flexors) can fail while activity in antagonist motoneurons (e.g., extensors) becomes tonic for a few step cycles (Lafreniere-Roula and McCrea, 2005). Deletions can be full (i.e., no activity in all synergists) or partial (reduced activity in some synergist motoneuron pools and no activity in others) (Lafreniere-Roula and McCrea, 2005). Examples of deletions are presented in Figs. 5A and B and will be discussed below. The key observation was that during many deletions, rhythmic motoneuron activity returned without phase shift following the deletion. It appeared that some internal structure could "remember" cycle period and the phase of locomotor oscillations when rhythmic motoneuron activity failed. A similar maintenance of cycle period has also been noted during studies of the effects of afferent stimulation on fictive locomotion (Guertin et al., 1995;Perreault et al., 1995;McCrea, 2001;Stecina et al., 2005). In such cases, afferent stimulation delays or causes a premature phase switching within the ongoing step cycle without changing the timing of the following step cycles. Examples of such effects of sensory stimulation and of deletions in which cycle timing is maintained are presented below. In order to reproduce such timing maintenance, we proposed an extension of the classical half-center CPG organization. We suggested that the locomotor CPG has a two-level architecture containing a half-center RG performing a "clock" function, and an intermediate pattern formation (PF) network containing interacting interneuron populations that activate multiple synergist and antagonist motoneuron pools (Lafreniere-Roula and McCrea, 2005;Rybak et al., 2006a,b). Conceptually, similar subdivisions of the mammalian CPG into separate networks for rhythm generation and motoneuron activation have been proposed previously (e.g., Koshland and Smith, 1989;Orsal et al., 1990;Kriellaars et al., 1994;Burke et al., 2001) but have not been formally modeled or considered in the context of non-resetting deletions and sensory stimulation (for discussion of a two-level CPG in the turtle see Lennard, 1985).

Figure 3A shows the schematic of our model of spinal circuitry with a two-level locomotor CPG (Rybak et al., 2006a, b). In the proposed architecture, the RG defines the locomotor rhythm and durations of flexor and extensor phases. It also controls activity in the PF network, which is responsible for activation and inhibition of flexor and extensor motoneurons. Each interneuron or motoneuron population in the model consists of 20 neurons simulated in Hodgkin-Huxley style. Motoneurons are described as two-compartment models (modified from Booth et al., 1997) and interneurons are simulated using single compartment models (Rybak et al., 2006a). The PF network contains excitatory interneuron populations projecting to motoneurons and to inhibitory interneurons within the PF network. A more complete locomotor model would have multiple PF populations to allow differential control of groups of motoneurons including those activating bifunctional muscles. In the reduced version of the model considered here, the PF network contains only two excitatory neural populations, PF-E and PF-F. Each of these populations receives a weak excitatory input from the homonymous RG population, strong inhibition from the opposite RG population via a corresponding inhibitory population (Inrg-E or Inrg-F) and reciprocal inhibition from the opposite PF population via another inhibitory population (Inpf-F or Inpf-E, see Fig. 3A). Locomotion is initiated in the model by external tonic excitation (from the "MLR") that is distributed to both the RG and PF populations (details in Rybak et al., 2006a).

Figure 3B shows examples of computer simulations of locomotor rhythm generation and flexor-and extensor-motoneuron activities. Alternating busts of activity in the RG-E and RG-F populations (evoked by MLR drive) produce periodic, alternating activity of the PF-E and PF-F populations which leads to rhythmic excitation of extensor (Mn-E) and flexor (Mn-F) motoneurons (bottom traces Fig. 3B). Variations in motoneuron excitability within each population (defined by the random distribution of leakage reversal potential and other neuronal

parameters) result in variations in firing rates and recruitment for a given level of PF drive to the population. This is shown in Fig. 3C (middle panel) by the raster plot of the firing in the 20 member flexor motoneuron population obtained from another simulation.

During fictive locomotion and in the absence of sensory activation by muscle spindle afferents, inhibitory Ia interneuron populations are phasically active (e.g., see Feldman and Orlovsky, 1975; McCrea et al., 1980; Pratt and Jordan, 1987) and since they are directly connected to motoneurons (Jankowska, 1992) they must contribute to the rhythmic inhibition of motoneurons. Accordingly, in our model PF activity excites inhibitory Ia-E and Ia-F interneurons (Fig. 3B, 5th and 6th traces from the top). The bottom trace in Fig. 3C is the simulated membrane potential from one flexor motoneuron showing the rhythmic depolarization and hyperpolarization (via Ia interneurons during extension) relative to the resting membrane potential (horizontal dashed line). The synaptic connections between IaINs, Renshaw cells, and motoneurons depicted in Fig. 3A are in accord with the known organization of this network (references in Jankowska, 1992). Thus during the active locomotor phase, motoneurons in the model receive both rhythmic excitation from the PF network and rhythmic inhibition from Renshaw cells (see RC-E and RC-F activities in Fig. 3B). During the opposite phase, they receive inhibition from the antagonist Ia population. Although the rhythmic inhibition of motoneurons is an important part of our model, we do not consider Ia inter-neurons or Renshaw cells to be part of the CPG. This is because they are not involved in rhythm generation per se and because their connections to motoneurons are organized on a more limited "local" basis (Jankowska, 1992). Thus the inhibition provided by sub-populations of these interneurons would sculpt the firing patterns of individual motoneuron pools during locomotion (Pratt and Jordan, 1987; Orlovsky et al., 1999). Recent evidence suggests that other as yet unidentified inter-neurons may also contribute to the rhythmic inhibition of motoneurons during locomotion (Gosgnach et al., 2006).

Control of cycle period and phase duration

Most of our simulations were carried out using fixed values for reciprocal inhibition, maximal conductance of NaP channels, and the maximal time constant for NaP channel inactivation (see Rybak et al., 2006a, b). These "standard" values (dots on the respective curves in Fig. 1C2–C4) were chosen to produce a cycle period on the order of 1 s. With these parameters fixed, a wide range of locomotor-cycle periods could be produced by varying the MLR drives to the RG populations (Fig. 1C1). Because of the symmetry of the two RG half-centers, equal MLR drive to both half-centers produced locomotor phases with equal durations. Unequal "flexor" and "extensor" phase durations could be produced by varying the drives to the RG-E and RG-F populations. Thus a stronger MLR drive to RG-E than to RG-F in Fig. 3B resulted in an extensor-phase dominated cycle, while increasing the MLR drive to the flexor circuitry in Fig. 3D produced a flexor phase-dominated rhythm with approximately the same locomotor-cycle period. Because motoneuron excitation is produced in the two-level CPG by the PF network, the level of motoneuron activity is similar in Fig. 3B and D. Although not shown, with a two-level CPG organization excitability changes at the PF level can strongly affect motoneuron activity and recruitment without changing locomotor-phase durations or step-cycle period.

In order to investigate the relative durations of the locomotor phases provided by the model, MLR drive was held constant in one RG population and progressively changed in the other. The thin lines in Fig. 4A1, A2, and B show the durations of the two locomotor phases obtained from the model in such experiments. In Fig. 4A1, reducing the drive to RG-E (d_{rge}) increased the duration of the flexion phase. Drive reduction had relatively little effect on the duration of the extension phase (i.e., the slope of the T_E line was shallow) but substantially prolonged the cycle period. In Fig. 4A2 and B, reducing drive to RG-F significantly prolonged the extension

(stance) phase with little effect on the flexor (swing) phase. In all three panels, decreasing excitation to one half-center had only a minor effect on the duration of activity in that half-center. Cycle period increased mainly because of the increased burst duration in the opposite RG population.

During both fictive and real locomotion, changes in cat step-cycle period often involve a disproportionate change in the duration of one of the phases. For example, during treadmill locomotion, faster cycle periods are made primarily at the expense of extensor phase duration (Fig. 4B, thick lines; data replotted from Halbertsma, 1983). As discussed elsewhere (Yakovenko et al., 2005), this asymmetry in phase duration modulation during real walking may result from the influence of particular proprioceptive feedback on the CPG. In the absence of rhythmic sensory feedback during fictive locomotion, some preparations show a similar change in extensor phase duration with cycle period (thick lines, Fig. 4A1, data from Yakovenko et al., 2005) while other preparations show preferential changes in the flexor phase (Fig. 4A2). We consider the fact that fictive locomotion can involve either a dominance of the flexor or extensor phase to be strong evidence for a CPG that is organized symmetrically with regard to its ability to control flexor- and extensor-phase durations (discussed in Lafreniere-Roula and McCrea, 2005;Duysens et al., 2006).

Insights into CPG organization from deletions of motoneuron activity during fictive locomotion

As mentioned, the stable alternation of flexor- and extensor-motoneuron activities during fictive locomotion can be briefly interrupted by periods in which motoneuron activity falls silent for a few step cycles and then reappears (e.g., Grillner and Zangger, 1979; Lafreniere-Roula and McCrea, 2005). Such spontaneously occurring errors or "deletions" of motoneuron activity also occur during the scratch reflex in turtles (see Stein, 2005) and during treadmill locomotion in cats (e.g., Duysens, 1977). When spontaneous deletions occur during MLR-evoked fictive locomotion or during fictive scratch, there is usually a failure of activity in multiple synergist motoneuron populations that is accompanied by tonic activity in multiple antagonist motoneuron populations (Lafreniere-Roula and McCrea, 2005). The widespread effect of deletions on the activity of multiple-motoneuron pools is strong evidence that they are produced by failures in the operation of some common spinal circuitry such as the CPG, and not the result of local perturbations affecting only the excitability of particular motoneurons.

An important feature of deletions concerns the timing of the locomotor bursts following a deletion episode. In the classical half-center CPG organization, a single network is responsible both for rhythm generation and motoneuron excitation. Accordingly, one would expect that a spontaneous deletion of motoneuron activity would be accompanied by changes in the timing of the locomotor RG. Since deletion duration could be arbitrary, post-deletion step cycles would often be expected to re-appear with a phase shift relative to the pre-deletion rhythm, i.e., the post-deletion rhythm would be reset. While "resetting" deletions do occur during fictive locomotion, it is more common for the post-deletion rhythm to be re-established without phase shift of the pre-deletion locomotor rhythm (Lafreniere-Roula and McCrea, 2005). The frequent occurrence of "non-resetting" deletions suggests that some internal structure can maintain locomotor period timing during the deletion of motoneuron activity.

Figure 5A and B, show examples of non-resetting deletions of flexor activity obtained during fictive locomotion. In Fig. 5A (from Lafreniere-Roula and McCrea, 2005) the failure of hip (Sart) and ankle (EDL) flexor motoneuron activation was accompanied by continuous activity of extensors operating at the hip (SmAB), knee (Quad), and ankle (Plant). The vertical dashed lines indicate intervals of the mean of the five-step cycle periods preceding the deletion. Note

that flexor activity re-appeared at a multiple of this interval. In other words, the rhythm is re-established with a timing that would have been expected had the deletion not occurred. During some of the expected bursts there was also a weak modulation of the sustained extensor-motoneuron activity (marked by *). Figure 5B shows a bout of MLR-evoked fictive locomotion with recordings from ipsi- and contralateral flexor and extensor nerves. During this recording there was a typical non-resetting deletion of ipsilateral flexor activity. Two bursts in the ipsilateral TA trace are omitted and this is accompanied by sustained firing of ipsilateral extensors, AB and LGS. Note that at this particular stage of the experiment, the contralateral nerves were not active (see coTA and coMG traces). This example demonstrates that maintenance of the phase of locomotor oscillations during non-resetting deletions does not require (and cannot be explained by) rhythmic activity in the contralateral hind limb (further discussion in Lafreniere-Roula and McCrea, 2005).

We suggest that deletions result from spontaneously occurring, temporary changes in the excitability of neurons in the RG or PF networks. First consider the effect of a relatively strong additional excitatory drive to one of the RG populations. An increase in excitability or an additional excitatory drive to one RG population can temporarily interrupt rhythm generation by producing sustained activity in this population and suppressing activity in the opposite RG half-center. Increased RG activity will also inhibit the opposite PF population, which then causes a deletion of the corresponding motoneuron activity. The rhythm will restart when the perturbation ends. However since the perturbation can end at an arbitrary time, the post-perturbation rhythm will likely be phase shifted (reset) with respect to the pre-deletion rhythm. Hence perturbations that change the excitability of the RG should generally produce the "resetting" type of deletion observed during fictive locomotion (Lafreniere-Roula and McCrea, 2005).

In contrast to the effects of altering excitability at the RG level, a temporary change in excitability of one of the PF populations can produce a deletion in which the phase of the post-deletion rhythm is maintained. The simulation in Fig. 5C shows the effects of a temporary increase in drive to the PF-E population (see the top trace). This increased drive results in sustained activity in the PF-E population and inhibition of activity in the opposite, PF-F, population. At the motoneuron level (two bottom traces in Fig. 5C), there is a deletion of flexor motoneuron activity with sustained activity of extensor motoneurons. An important feature of this deletion is the lack of resetting of the post-deletion rhythm. Because RG operation is unchanged during the deletion, motoneuron activity re-appears without a phase shift. Note the weak rhythmic modulation of extensor motoneuron activity during the periods where flexor bursts "should" have occurred (vertical dashed lines). This is similar to that observed in experimental records (see Fig. 5A). In the model, the weak modulation of sustained motoneuron activity is the result of continued rhythmic activity at the RG level. In the example shown, RG-F inhibition produces a periodic modulation of PF-E activity that is reflected at the motoneuron level. Simulations of other types of deletions using the model are described in Rybak et al. (2006a). These modeling studies show that the proposed two-level CPG architecture can readily account for both the resetting and non-resetting types of deletions observed during fictive locomotion in the cat.

Afferent control of the CPG at the PF and RG levels

Although the spinal CPG can operate in the absence of sensory feedback (e.g., during fictive locomotion) afferent activity plays a critical role in adjusting the locomotor pattern to the motor task, environment, and biomechanical characteristics of the limbs and body (Pearson, 2004; Rossignol et al., 2006). To illustrate the effects of afferent stimulation on motoneuron activity during locomotion in the context of the two-level CPG organization considered here, we will consider the effects of activation of the extensor group I (Ia muscle spindle and Ib tendon organ)

afferents. Modeling the effects of stimulation of other afferents (i.e., flexor and cutaneous) can be found in Rybak et al. (2006b).

A large body of experimental evidence shows that proprioceptive feedback from extensor group I afferents, and particularly those from ankle muscle nerves, results in a strong excitation of extensor motoneurons that contributes to a substantial portion of stance-phase extensor activity in cats during treadmill locomotion (see Donelan and Pearson, 2004; Rossignol et al., 2006), and in man (Sinkjaer et al., 2000). In reduced preparations, activity in extensor group I afferents can also control the transition from stance to swing, regulate the duration of the stance phase, and entrain the step-cycle period (see Guertin et al., 1995; Pearson, 2004; Rossignol et al., 2006).

Figure 6 shows the schematic of the extended model used to simulate control of locomotor pattern by group I extensor afferents. During locomotion, extensor group I afferents can access the spinal circuitry at several levels. The model includes monosynaptic excitation of homonymous motoneurons and disynaptic inhibition of antagonists by group Ia afferents. The weight of Ia monosynaptic excitation has been made low to reflect the presynaptic inhibition of these afferents during locomotion (Gosgnach et al., 2000;McCrea, 2001). The model also includes the locomotor-dependent disynaptic excitation of motoneurons (see Angel et al., 2005) that is mediated by the excitatory population Iab-E. During extension (i.e., when PF-E and Inpf-F are active), the Inpf-F population inhibits In-E thereby removing the In-E inhibition of Iab-E. This disinhibition permits a phase-dependent disynaptic excitation of extensors by group I extensor afferents (Schomburg and Behrends, 1978;McCrea et al., 1995;Angel et al., 1996,2005). In addition, excitation of the Iab-E population from the PF-E population creates rhythmic extensor-phase activity in Iab-E inter-neurons in the absence of sensory stimulation that is in accord with that found experimentally (Angel et al., 2005). Thus these Iab-E interneurons also provide a portion of the excitation of extensor motoneurons during locomotion. Nonetheless, we do not consider the Iab-E population to be an integral part of the CPG. This is because they do not participate in rhythm generation and in some locomotor preparations, their excitability is low and group I disynaptic excitation motoneurons cannot be evoked (e.g., low spinal cats, McCrea et al., 1995). A more complete discussion of how group I disynaptic excitation emerges during locomotion and replaces the inhibitory effects evoked at rest is presented elsewhere (Rybak et al., 2006b).

Additional interneuron populations have been added to the model to mediate the effects of extensor group I afferents on the CPG during locomotion (references in McCrea, 2001; Pearson, 2004; Rossignol et al., 2006). In the framework of the two-level CPG, we have hypothesized that there are separate pathways for extensor group I excitation through the RG and the PF levels of the CPG via the hypothetical Irg-E and Ipf-E populations, respectively (Fig. 6). According to the suggestion explored here, the synaptic weight of group I input to the PF-E population (controlling extensor activity at the PF level) is stronger than that to RG-E (the extensor half-center of the RG).

Figure 7A1 and A2 shows two examples of simulations of the effects of a short duration stimulus to extensor group I afferents during the extension phase of locomotion, i.e., when both the RG-E and PF-E populations are active. With the moderate intensity stimulation in Fig. 7A1, there was only a small effect on RG population activity. Hence this afferent stimulation did not change the locomotor rhythm generated by the RG (see the second and third traces in Fig. 7A1). The stimulation did, however, enhance and prolong PF-E population activity, which in turn enhanced and prolonged the activity of extensor motoneurons (Fig. 7A1, bottom trace). The prolongation in PF-E activity delayed the switching to the flexion phase at the PF-F level (see fourth and fifth traces in Fig. 7A1). However, because the RG was not affected, the subsequent flexion phase was shortened and the duration of the ongoing step cycle remained

constant. This is consistent with the experimental data shown in Fig. 7B1 where plantaris nerve stimulation enhanced and prolonged extensor motoneuron activity (hip: AB, knee: Quad, and ankle: MG). As in our simulation, there was a corresponding shortening of the subsequent flexor phase such that the ongoing step-cycle period remained unchanged (see arrows at the bottom of Fig. 7B1).

In Fig. 7A2 the intensity of stimulation is three times stronger than that in Fig. 7A1. Unlike the weaker stimulation, this stimulation also increased RG-E activity, which in turn delayed the transition to flexion (see second and third traces in Fig. 7A2). The net effect was an increase and prolongation of extensor motoneuron firing (see the bottom trace in Fig. 7A2). There was, however, no compensatory change in the duration of the subsequent flexor phase. Consequently, each stimulus prolonged the duration of the ongoing locomotor cycle and hence produced a phase shift of the post-stimulation rhythm. An experimental example of a group I extensor stimulation-evoked enhancement and prolongation of extensor motoneuron activity in which the ongoing step-cycle period was increased is shown in Fig. 7B2. In this example, each stimulus applied to group I extensor afferents (Sm, a hip extensor) enhanced and prolonged extensor (MG) bursts. The following flexor phase had an unchanged duration and hence the locomotor rhythm was shifted in time (see arrows at the bottom of the figure).

Based on the results of these simulations, we conclude that stimulation of group I extensor afferents during extension may prolong and enhance activity during the current extension phase, with or without changing the duration of ongoing locomotor cycle and the phase of post-stimulation rhythm. The exact effect in the model depends on how strongly the applied stimulation influences the RG. With separate access of proprioceptive feedback to the RG and the PF networks, the contribution of extensor group I afferents to weight support and the control of stance-swing transitions may be accomplished via separate pathways within the CPG. Specifically we hypothesize that enhanced weight support (i.e., level of extensor motoneuron activity) during stance can be provided by the PF network, while actions on the extensor portion of the RG can control the timing of stance to swing transitions.

Conclusions

Development of the present CPG model began with observations obtained during fictive locomotion in the cat showing that cycle phase could be maintained during deletions and during sensory stimulation. This phase maintenance necessitated consideration of a two-level CPG in which the tasks of rhythm generation and motoneuron activation were separate since such phase maintenance is not easily accommodated within the classical half-center CPG concept. The RG structure and the parameters of RG neurons were selected to be able to reproduce the range of locomotor-cycle periods and phase durations observed during fictive and treadmill locomotion. Modeling shows that this two-level CPG architecture consisting of a half-center RG and a PF network can replicate and explain the existence of resetting and non-resetting deletions. The same model can also realistically reproduce the actions of reflex circuits during locomotion and provide explanations for the effects of afferent stimulation on CPG observed experimentally. We believe that analysis of "mistakes" and sensory perturbations of CPG operation in the fictive locomotion preparation has provided a unique insight into the structure of the CPG operating during real locomotion.

Finally, we must stress that the present model is a work in progress. As more experimental data becomes available, the model will need to be modified to reproduce CPG activity observed under other conditions. Extensions to the model will include incorporating more than two motoneuron pools and adding more sources of sensory and descending control to the CPG.

We also hope that the model may assist in the development of criteria for the functional identification of spinal interneuron classes involved in locomotor pattern and rhythm generation. For example, based on the model, we suggest that excitatory RG neurons should have the following features. These neurons should (i) receive excitation from the MLR region, (ii) demonstrate rhythmic activity during fictive locomotion that persists during non-resetting deletions, and (iii) not be monosynaptically coupled to motoneurons. In contrast, the neurons comprising the PF network should (i) demonstrate rhythmic activity during fictive locomotion that fails during non-resetting deletions and (ii) produce monosynaptic EPSPs in synergist motoneurons. Even a partial experimental identification of some of the classes of CPG neurons postulated in the model would provide opportunities to directly examine the intrinsic cellular properties underlying rhythm generation in the adult mammalian spinal cord.

References

Akay T, McVea DA, Tachibana A, Pearson KG. Coordination of fore and hind leg stepping in cats on a transversely-split treadmill. Exp Brain Res 2006;175:211–222. [PubMed: 16733696]

Angel MJ, Guertin P, Jiminez I, McCrea DA. Group I extensor afferents evoke disynaptic EPSPs in cat hindlimb extensor motoneurones during fictive locomotion. J Physiol 1996;494:851–861. [PubMed: 8865080]

Angel MJ, Jankowska E, McCrea DA. Candidate interneurones mediating group I disynaptic EPSPs in extensor motoneurons during fictive locomotion in the cat. J Physiol 2005;563(Pt 2):597–610. [PubMed: 15618278]

Beato M, Nistri A. Interaction between disinhibited bursting and fictive locomotor patterns in the rat isolated spinal cord. J Neurophysiol 1999;82:2029–2038. [PubMed: 10561384]

Booth V, Rinzel J, Kiehn O. Compartmental model of vertebrate motoneurons for Ca^{2+}-dependent spiking and plateau potentials under pharmacological treatment. J Neurophysiol 1997;78:3371–3385. [PubMed: 9405551]

Brocard FF, Tazerart S, Viermari JC, Darbon P, Vinay L. Persistent sodium inward current (INaP) in the neonatal rat lumbar spinal cord and its contribution to locomotor pattern generation. Soc Neurosci Abstr 2006:252.16.

Burke RE, Degtyarenko AM, Simon ES. Patterns of locomotor drive to motoneurons and last-order interneurons: clues to the structure of the CPG. J Neurophysiol 2001;86:447–462. [PubMed: 11431524]

Büschges A, Wikstroöm MA, Grillner S, El Manira A. Roles of high-voltage activated calcium channel subtypes in a vertebrate spinal locomotor network. J Neurophysiol 2000;84:2758–2766. [PubMed: 11110806]

Butera RJ, Rinzel JR, Smith JC. Models of respiratory rhythm generation in the pre-Bötzinger complex: I. Bursting pacemaker neurons. J Neurophysiol 1999a;82:382–397. [PubMed: 10400966]

Butera RJ, Rinzel JR, Smith JC. Models of respiratory rhythm generation in the pre-Bötzinger complex: II. Populations of coupled pacemaker neurons. J Neurophysiol 1999b;82:398–415. [PubMed: 10400967]

Butt SJB, Harris-Warrick RM, Kiehn O. Firing properties of identified interneuron populations in the mammalian hindlimb central pattern generator. J Neurosci 2002;22:9961–9971. [PubMed: 12427853]

Cowley KC, Schmidt BJ. Effects of inhibitory amino acid antagonists on reciprocal inhibitory interactions during rhythmic motor activity in the in vitro neonatal rat spinal cord. J Neurophysiol 1995;74:1109–1117. [PubMed: 7500136]

Dai Y, Jordan LM. Characterization of persistent inward currents (PICs) in locomotor activity-related neurons of Cfos-EGFP mice. Soc Neurosci Abstr 2006:130.6.

Darbon P, Yvon C, Legrand JC, Streit J. INaP underlies intrinsic spiking and rhythm generation in networks of cultured rat spinal cord neurons. Eur J Neurosci 2004;20:976–988. [PubMed: 15305866]

Dietz V. Spinal cord pattern generators for locomotion. Clin Neurophysiol 2003;114:1379–1389. [PubMed: 12888019]

Donelan JM, Pearson KG. Contribution of force feedback to ankle extensor activity in decerebrate walking cats. J Neurophysiol 2004;92:2093–2104. [PubMed: 15381742]

Duysens J. Reflex control locomotion as revealed by stimulation of cutaneous afferents in spontaneously walking premammillary cats. J Neurophysiol 1977;40:737–751. [PubMed: 886369]

Duysens J, McCrea D, Lafreniere-Roula M. How deletions in a model could help explain deletions in the laboratory. J Neurophysiol 2006;95:562–565. [PubMed: 16339509]

El Manira A, Tegner J, Grillner S. Calcium-dependent potassium channels play a critical role for burst termination in the locomotor network in lamprey. J Neurophysiol 1994;72:1852–1861. [PubMed: 7823105]

Fedirchuk B, Dai Y. Monoamines increase the excitability of spinal neurones in the neonatal rat by hyperpolarizing the threshold for action potential production. J Physiol 2004;557:355–361. [PubMed: 15090607]

Feldman AG, Orlovsky GN. Activity of inter-neurons mediating reciprocal Ia inhibition during locomotion. Brain Res 1975;84:181–194. [PubMed: 1111829]

Forssberg H, Grillner S, Halbertsma J, Rossignol S. The locomotion of the low spinal cat: II. Interlimb coordination. Acta Physiol Scand 1980;108:283–295. [PubMed: 7376923]

Gosgnach S, Lanuza GM, Butt SJ, Saueressig H, Zhang Y, Velasquez T, Riethmacher D, Callaway EM, Kiehn O, Goulding M. V1 spinal neurons regulate the speed of vertebrate locomotor outputs. Nature 2006;440:215–219. [PubMed: 16525473]

Gosgnach S, Quevedo J, Fedirchuk B, McCrea DA. Depression of group Ia monosynaptic EPSPs in cat hindlimb motoneurones during fictive locomotion. J Physiol 2000;526:639–652. [PubMed: 10922014]

Graham Brown T. On the fundamental activity of the nervous centres: together with an analysis of the conditioning of rhythmic activity in progression, and a theory of the evolution of function in the nervous system. J Physiol 1914;48:18–41. [PubMed: 16993247]

Grillner, S. Control of locomotion in bipeds, tetrapods, and fish. In: Brookhart, JM.; Mountcastle, VB., editors. Handbook of Physiology. The Nervous System. Motor Control, Sect 1. II. American Physiological Society; Bethesda, MD: 1981. p. 1179-1236.

Grillner S. The motor infrastructure: from ion channels to neuronal networks. Nat Rev Neurosci 2003;4:573–586. [PubMed: 12838332]

Grillner S, Wallén P. Cellular bases of a vertebrate locomotor system-steering, intersegmental and segmental co-ordination and sensory control. Brain Res Rev 2002;40:92–106. [PubMed: 12589909]

Grillner S, Wallén P, Hill R, Cangiano L, El Manira A. Ion channels of importance for the locomotor pattern generation in the lamprey brainstem-spinal cord. J Physiol 2001;533:23–30. [PubMed: 11351009]

Grillner S, Zangger P. On the central generation of locomotion in the low spinal cat. Exp Brain Res 1979;34:241–261. [PubMed: 421750]

Guertin P, Angel MJ, Perreault MC, McCrea DA. Ankle extensor group I afferents excite extensors throughout the hindlimb during fictive locomotion in the cat. J Physiol 1995;487:197–209. [PubMed: 7473249]

Halbertsma JM. The stride cycle of the cat: the modelling of locomotion by computerized analysis of automatic recordings. Acta Physiol Scand Suppl 1983;521:1–75. [PubMed: 6582764]

Jankowska E. Interneuronal relay in spinal pathways from proprioceptors. Prog Neurobiol 1992;38:335–378. [PubMed: 1315446]

Kiehn O. Locomotor circuits in the mammalian spinal cord. Annu Rev Neurosci 2006;29:279–306. [PubMed: 16776587]

Kjaerulff O, Kiehn O. 5-HT modulation of multiple inward rectifiers in motoneurons in intact preparations of the neonatal rat spinal cord. J Neurophysiol 2001;85:580–593. [PubMed: 11160495]

Koshland GF, Smith JL. Mutable and immutable features of paw-shake responses after hindlimb deafferentation in the cat. J Neurophysiol 1989;62:162–173. [PubMed: 2754470]

Kremer E, Lev-Tov A. GABA-receptor-independent dorsal root afferents depolarization in the neonatal rat spinal cord. J Neurophysiol 1998;79:2581–2592. [PubMed: 9582230]

Kriellaars DJ, Brownstone RM, Noga BR, Jordan LM. Mechanical entrainment of fictive locomotion in the decerebrate cat. J Neurophysiol 1994;71:2074–2086. [PubMed: 7931503]

Lafreniere-Roula M, McCrea DA. Deletions of rhythmic motoneuron activity during fictive locomotion and scratch provide clues to the organization of the mammalian central pattern generator. J Neurophysiol 2005;94:1120–1132. [PubMed: 15872066]

Lee RH, Heckman CJ. Essential role of a fast persistent inward current in action potential initiation and control of rhythmic firing. J Neurophysiol 2001;85:472–475. [PubMed: 11152749]

Lennard PR. Afferent perturbations during "monopodal" swimming movements in the turtle: phase-dependent cutaneous modulation and proprioceptive resetting of the locomotor rhythm. J Neurosci 1985;5:1434–1445. [PubMed: 4009241]

Lundberg, A. Half-centres revisited. In: Szentagothai, J.; Palkovits, M.; Hamori, J., editors. Regulatory Functions of the CNS Motion and Organization Principles. Pergamon Akadem Kiado; Budapest, Hungary: 1981. p. 155-167.

McCrea DA. Spinal circuitry of sensorimotor control of locomotion. J Physiol 2001;533:41–50. [PubMed: 11351011]

McCrea DA, Pratt CA, Jordan LM. Renshaw cell activity and recurrent effects on motoneurons during fictive locomotion. J Neurophysiol 1980;44:475–488. [PubMed: 7441311]

McCrea DA, Shefchyk SJ, Stephens MJ, Pearson KG. Disynaptic group I excitation of synergist ankle extensor motoneurones during fictive locomotion in the cat. J Physiol 1995;487:527–539. [PubMed: 8558481]

Miller S, van der Meche FG. Coordinated stepping of all four limbs in the high spinal cat. Brain Res 1976;109:395–398. [PubMed: 1276923]

Noga BR, Cowley KC, Huang A, Jordan LM, Schmidt BJ. Effects of inhibitory amino acid antagonists on locomotor rhythm in the decerebrate cat. Soc Neurosci Abstr 1993:225.4.

Orlovsky, GN.; Deliagina, T.; Grillner, S. Neuronal control of locomotion: from mollusc to man. Oxford University Press; New York: 1999.

Orsal D, Cabelguen JM, Perret C. Interlimb coordination during fictive locomotion in the thalamic cat. Exp Brain Res 1990;82:536–546. [PubMed: 2292272]

Paton JFR, Abdala APL, Koizumi H, Smith JC, John WM. Respiratory rhythm generation during gasping depends on persistent sodium current. Nat Neurosci 2006;9:311–313. [PubMed: 16474390]

Pearson KG. Generating the walking gait: role of sensory feedback. Prog Brain Res 2004;143:123–129. [PubMed: 14653157]

Perreault MC, Angel MJ, Guertin P, McCrea DA. Effects of stimulation of hindlimb flexor group II afferents during fictive locomotion in the cat. J Physiol 1995;487:211–220. [PubMed: 7473250]

Perrier JF, Alaburda A, Hounsgaard J. 5-HT1A receptors increase excitability of spinal motoneurons by inhibiting a TASK-1-like K+ current in the adult turtle. J Physiol 2003;548:485–492. [PubMed: 12626670]

Pratt CA, Jordan LM. Ia inhibitory interneurons and Renshaw cells as contributors to the spinal mechanisms of fictive locomotion. J Neurophysiol 1987;57:56–71. [PubMed: 3559681]

Rossignol, S. Neural control of stereotypic limb movements. In: Rowell, LB.; Shepherd, J., editors. Handbook of Physiology, Sect 12. The American Physiological Society; Bethesda, MD: 1996. p. 173-216.

Rossignol S, Dubuc R, Gossard JP. Dynamic sensorimotor interactions in locomotion. Physiol Rev 2006;86:89–154. [PubMed: 16371596]

Rybak IA, Shevtsova NA, Lafreniere-Roula M, McCrea DA. Modelling spinal circuitry involved in locomotor pattern generation: insights from deletions during fictive locomotion. J Physiol 2006a; 577:617–639. [PubMed: 17008376]

Rybak IA, Shevtsova NA, Ptak K, McCrimmon DR. Intrinsic bursting activity in the pre-Bötzinger complex: role of persistent sodium and potassium currents. Biol Cybern 2004;90:59–74. [PubMed: 14762725]

Rybak IA, Shevtsova NA, John WM, Paton JFR, Pierrefiche O. Endogenous rhythm generation in the pre-Böztzinger complex and ionic currents: modelling and in vitro studies. Eur J Neurosci 2003;18:239–257. [PubMed: 12887406]

Rybak IA, Stecina K, Shevtsova NA, McCrea DA. Modelling spinal circuitry involved in locomotor pattern generation: insights from the effects of afferent stimulation. J Physiol 2006b;577:641–658. [PubMed: 17008375]

Schomburg ED, Behrends HB. The possibility of phase-dependent monosynaptic and polysynaptic Ia excitation to homonymous motoneurones during fictive locomotion. Brain Res 1978;143:533–537. [PubMed: 647377]

Sinkjaer T, Andersen JB, Ladouceur M, Christensen LOD, Nielsen J. Major role for sensory feedback in soleus EMG activity in the stance phase of walking in man. J Physiol 2000;523:817–827. [PubMed: 10718758]

Sirota MG, Shik ML. The cat locomotion elicited through the electrode implanted in the mid-brain. Sechenov Physiol J USSR 1973;59:1314–1321.(in Russian)

Smith JC, Butera RJ, Koshiya N, Del Negro C, Wilson CG, Johnson SM. Respiratory rhythm generation in neonatal and adult mammals: the hybrid pacemaker-network model. Respir Physiol 2000;122:131–147. [PubMed: 10967340]

Stecina K, Quevedo J, McCrea DA. Parallel reflex pathways from flexor muscle afferents evoking resetting and flexion enhancement during fictive locomotion and scratch in the cat. J Physiol 2005;569:275–290. [PubMed: 16141269]

Stein PSG. Neuronal control of turtle hindlimb motor rhythms. J Comp Physiol A 2005;191:213–229.

Stein, PSG.; Smith, JL. Neural and biomechanical control strategies for different forms of vertebrate hindlimb motor tasks. In: Stein, P.; Grillner, S.; Selverston, AI.; Stuart, DG., editors. Neurons, Networks, and Motor Behavior. MIT Press; Cambridge, MA: 1997. p. 61-73.

Streit, J.; Tscherter, A.; Darbon, P. Advances in Neural Information Processing Systems. Springer; New York: 2006. Rhythm generation in spinal culture: Is it the neuron or the network?; p. 377-408.

Theiss RD, Kuo JJ, Heckman CJ. Persistent inward currents in rat ventral horn neurons. J Physiol 2007;580:507–522. [PubMed: 17289788]

Yakovenko S, McCrea DA, Stecina K, Prochazka A. Control of locomotor cycle durations. J Neurophysiol 2005;94:1057–1065. [PubMed: 15800075]

Yamaguchi T. The central pattern generator for forelimb locomotion in the cat. Prog Brain Res 2004;143:115–122. [PubMed: 14653156]

Yang JF, Lam T, Pang MY, Lamont E, Musselman K, Seinen E. Infant stepping: a window to the behaviour of the human pattern generator for walking. Can J Physiol Pharmacol 2004;82:662–674. [PubMed: 15523523]

Zehr EP, Duysens J. Regulation of arm and leg movement during human locomotion. Neuroscientist 2004;10:347–361. [PubMed: 15271262]

Zhong G, Masino MA, Harris-Warrick RM. Persistent sodium currents participate in fictive locomotion generation in neonatal mouse spinal cord. Soc Neurosci Abstr 2006:128.17.
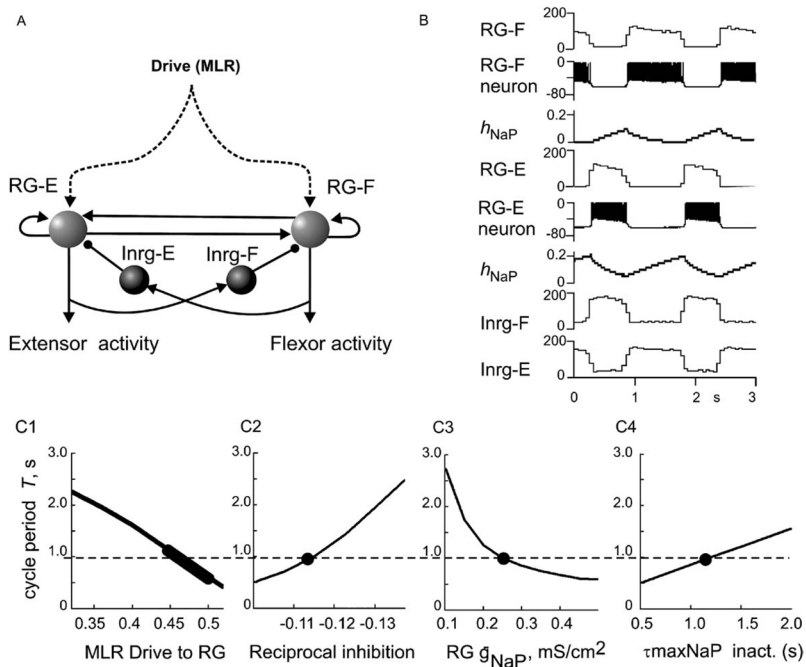
Fig. 1.
Operation of the locomotor rhythm generator (RG). (A) Model Schematic. Each sphere
represents a 20-neuron population. Excitatory and inhibitory synaptic connections are shown
by arrows and small circles, respectively. Excitatory drive (from the MLR) is shown by dashed
lines. The RG consists of two populations of excitatory neurons (RG-E and RG-F)
interconnected via inhibitory interneuron populations, Inrg-E and Inrg-F, and mutual excitatory
connections. (B) Activity of RG populations during two-step cycles. The top three traces for
the flexor population show, respectively, the histogram of average RG-F neuron activity, the
membrane potential trajectory in one RG-F neuron, and change in the inactivation variable for
persistent (slowly inactivating) sodium (NaP) channel (h_{NaP}) in this neuron. The next three
traces show the corresponding variables for the extensor portion of the RG. Activities of
inhibitory interneuron populations, Inrg-F and Inrg-E, are shown in the two bottom traces. In
this and other figures, population activity is represented by a histogram of average firing
frequency (number of spikes per second per neuron, bin = 30 ms). (C) Dependence of locomotor
step-cycle period on model parameters. (C1) Increased drive to both RG populations (indicated
by arbitrary units on in the horizontal axis) reduces step-cycle period (T). (C2) Step-cycle
period monotonically increases with an increase in mutual inhibition between the RG
populations. Mutual inhibition was increased (see abscissa) by an increase in the weight of
inhibitory synaptic input from Inrg-E and Inrg-F to their respective targets. (C3) T
monotonically decreases with an increase of the maximal conductance of persistent sodium
(NaP) channels in RG neurons (g_{NaP}). (C4) Increasing the time constant for NaP channel
inactivation (τ_{maxNaP}) causes a linear increase in T. The dots in C2–C4 and the heavy line in
C1 indicate values of these parameters used for most simulations.
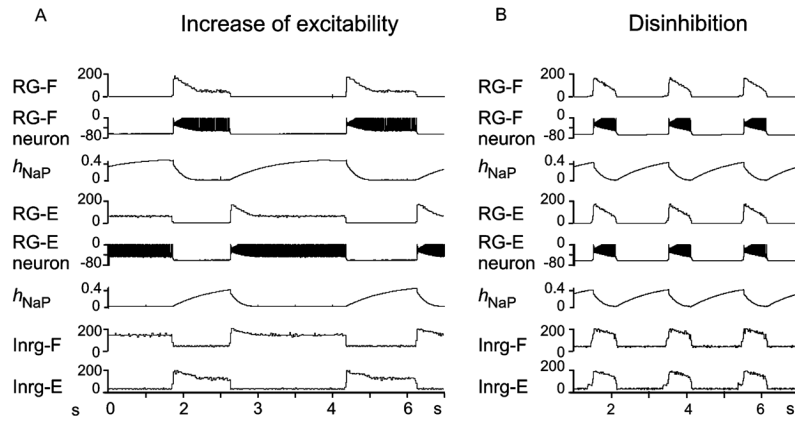
Fig. 2.
Rhythms in the absence of MLR drive. (A) Imitation of pharmacologically evoked rhythm in the model. The slow rhythmic activity was produced by an increase in excitability of the excitatory RG populations in the absence of external (MLR) drive. This increased excitability was produced by a 6 mV depolarization of the average leakage reversal potential in all neurons of these populations. (B) Rhythmic activity produced in the model by disinhibiton. To simulate this behavior, the weights of all inhibitory connection in the model were set to zero. Note the synchronized rhythmic bursts of flexors and extensors. See details in the text. Figure adapted with permission from Rybak et al. (2006a)
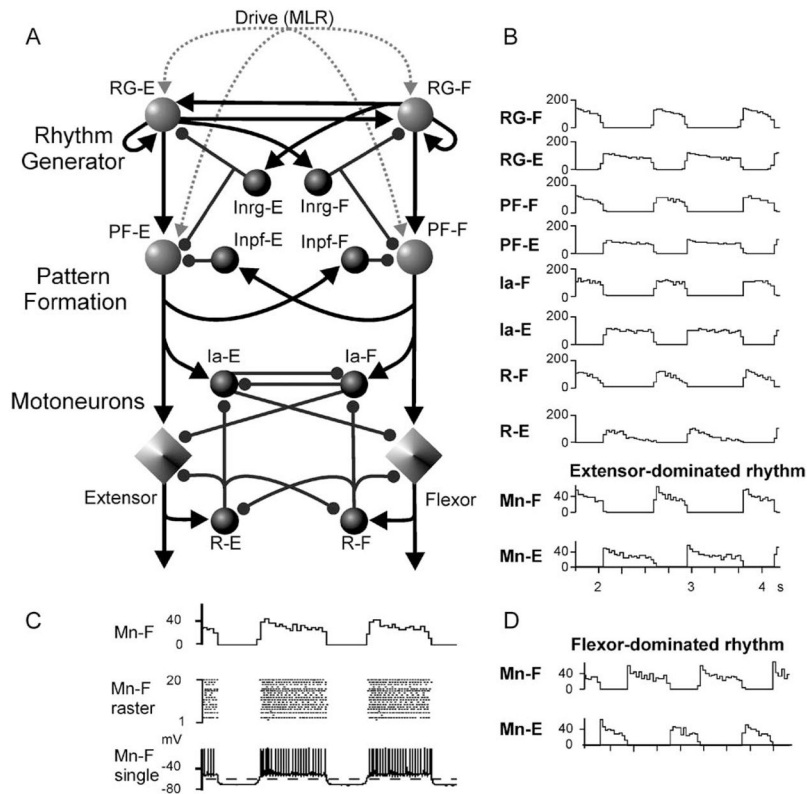
Fig. 3.
Model of spinal circuitry with a two-level locomotor CPG without afferent inputs. (A) Schematic of the model. Populations of interneurons are represented by spheres. Excitatory and inhibitory synaptic connections are shown by arrows and small circles, respectively. Populations of flexor (Mn-F) and extensor (Mn-E) motoneurons are shown by diamonds. MLR excitatory drives are shown as dashed lines. See explanations in the text. (B) Locomotor activity patterns generated by the model. Activity of each population is represented by a histogram of average firing frequency. The MLR drive to the RG-E population (d_{rge} = 0.5 arbitrary units) is larger than to RG-F population (d_{rgf} = 0.43) and the model generates a rhythm with a longer duration extensor phase ($T_E > T_F$). In D, the RG-F population receives a larger drive (d_{rgf} = 0.51; d_{rge} = 0.45) and the model generates a flexion-dominated rhythm ($T_F > T_E$). Figure adapted with permission from Rybak et al. (2006a). (C) Flexor motoneuron population firing activity obtained in another simulation (upper trace), raster plot of spiking activity in the population (middle) and the trace of the membrane potential from a single flexor motoneuron. Note the rhythmic hyperpolarization of the motoneuron below resting membrane potential (horizontal dashed line) during the extension phase.
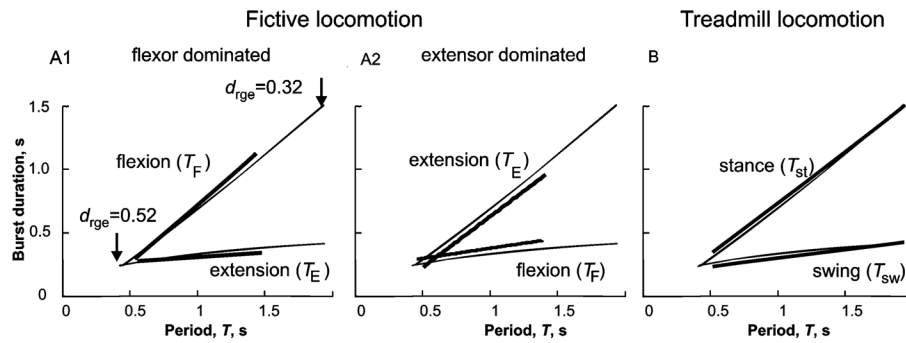
Fig. 4.
Comparison of simulated locomotor-phase and step-cycle durations to experimental data. Thin lines in the three panels show the durations of simulated flexor and extensor phases plotted against the step-cycle period on the abscissa. These plots were created by holding the MLR drive to one side of the RG constant (RG-F in A1 and RG-E in A2 and B) and varying the drive to the other side of the RG. In A1, the flexor drive (d_{rgf}) was held constant at 0.52 (arbitrary units) and the extensor drive (d_{rge}) decreased from 0.52 to 0.32. The inverse of this procedure (i.e., holding d_{rge} constant) produced the simulations curves in A2 and B. Note that an increase in d_{rge} speeds up locomotion mainly by decreasing the duration of the opposite (flexor) phase, T_F with little effect on T_E. See text for explanation. The bold lines in the three panels are linear regressions of measurements of cycle phase duration for fictive locomotion in decerebrate cats (A1 and A2, data from Yakovenko et al., 2005) and for treadmill locomotion in intact cats (data from Halbertsma, 1983). The fictive locomotion data is separated into measurements from experiments in which the flexion phase dominated the fictive locomotor pattern (A1), and from those in which extensor activity was longer (A2) (see Yakovenko et al., 2005). Note the close correspondence between actual and modeled phase duration plots for both the duration of extensor (T_E) and flexor (T_F) nerve activity (A1 and A2) during fictive locomotion and for the durations of the stance (T_{st}) and swing phases (T_{sw}) during real locomotion. Adapted with permission from Rybak et al. (2006a).
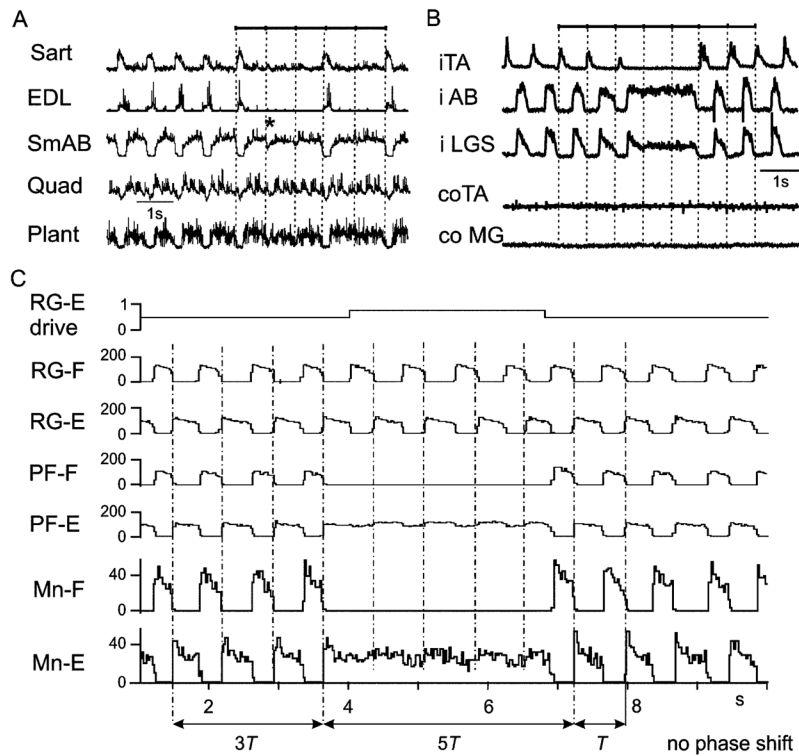
Fig. 5.
Examples of deletions occurring during MLR-evoked fictive locomotion and simulation of "non-resetting" deletions. (A) An example of a deletion of flexor activity during fictive locomotion. The traces are rectified-integrated recordings from hindlimb flexors (hip: Sart and ankle: EDL) and extensors (hip: SmAB, knee: Quad, and ankle: Plant). The vertical dashed lines are plotted at intervals of the average cycle period preceding the deletions and indicate where flexor bursts should have occurred. Note the re-emergence of flexor activity at these intervals following the deletion. The * indicates a weak modulation of the sustained extensor motoneuron activity. Adapted with permission from Lafreniere-Roula and McCrea (2005). (B) Another example of deletion of flexor activity in which there was no contralateral flexor and extensor activity (see coTA and coMG traces). The non-resetting deletion of ipsilateral flexor activity (iTA) was accompanied by sustained firing of ipsilateral extensors (iAB and iLGS). Vertical dashed lines show that the phase of the locomotor rhythm is maintained after the deletion despite the absence of contralateral locomotor activity. (C) Simulation of the deletion of flexor activity in A produced by a temporary 90% increase in excitatory drive to the PF-E population (top trace). This drive produced sustained PF-E population activity and consequently sustained activity in the Mn-E population. Inhibition of the PF-F population resulted in a deletion of flexor motoneuron activity. The vertical dashed lines show that the rhythm re-appeared without a phase shift in respect to the pre-deletion rhythm (see arrows at the bottom of each panel). Adapted with permission from Rybak et al. (2006a).
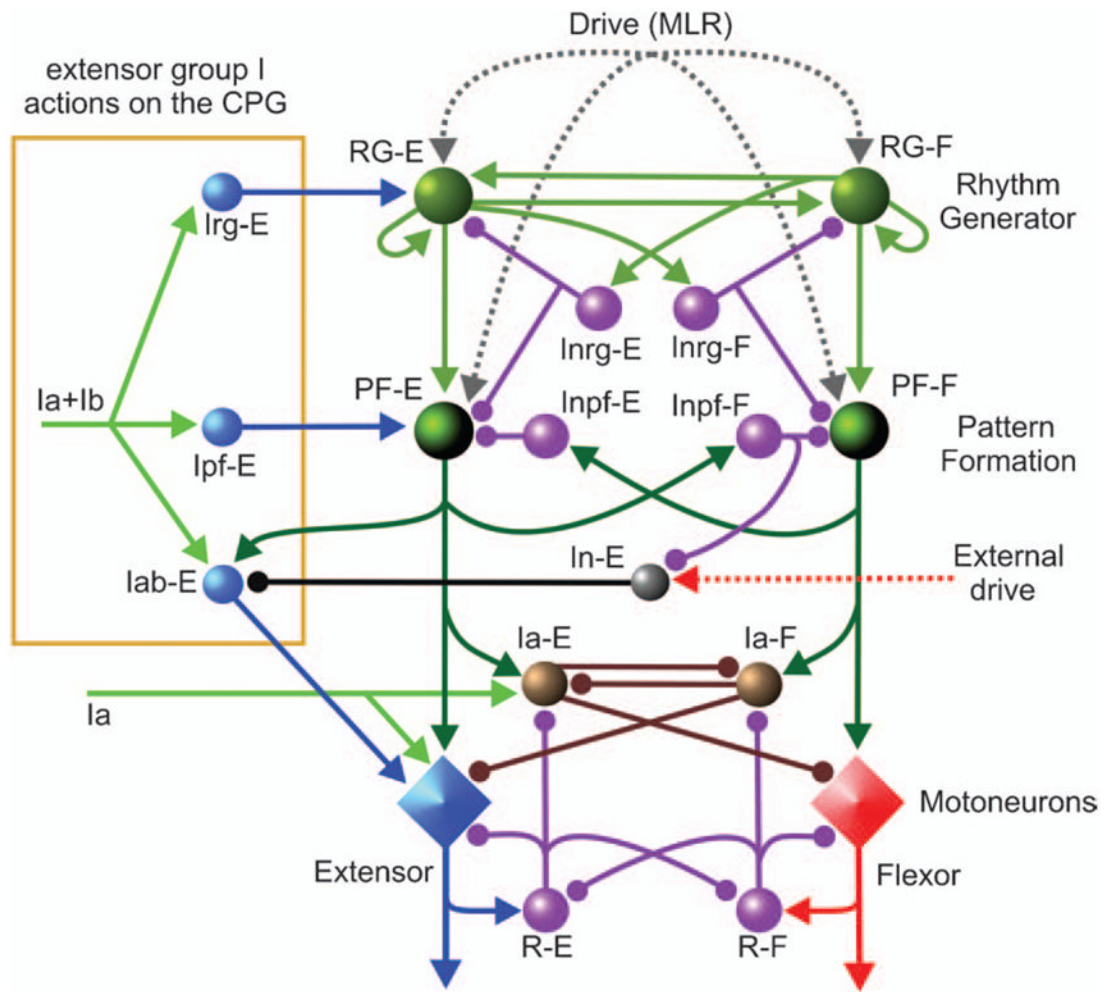
Fig. 6.
Model schematic of the spinal cord circuitry integrated with the locomotor CPG used for simulation of the effects of extensor group I afferent stimulation during fictive locomotion. This model extends that shown in Fig. 3A to include pathways for group I extensor afferents. Connections of group I (Ia and Ib) extensor afferents are shown on the left. Interneuron populations Irg-E and Ipf-E mediate the access of extensor group I (Ia and Ib) afferents to the rhythm generator (RG-E) and the pattern formation (PF-E) networks, respectively. The Iab-E and In-E populations provide phase-dependent disynaptic excitation of extensor motoneurons by group I extensor afferents. During the extensor phase of fictive locomotion, the Iab-E population is released from inhibition of In-E and mediates disynaptic excitation of extensor motoneurons. See details in the text.
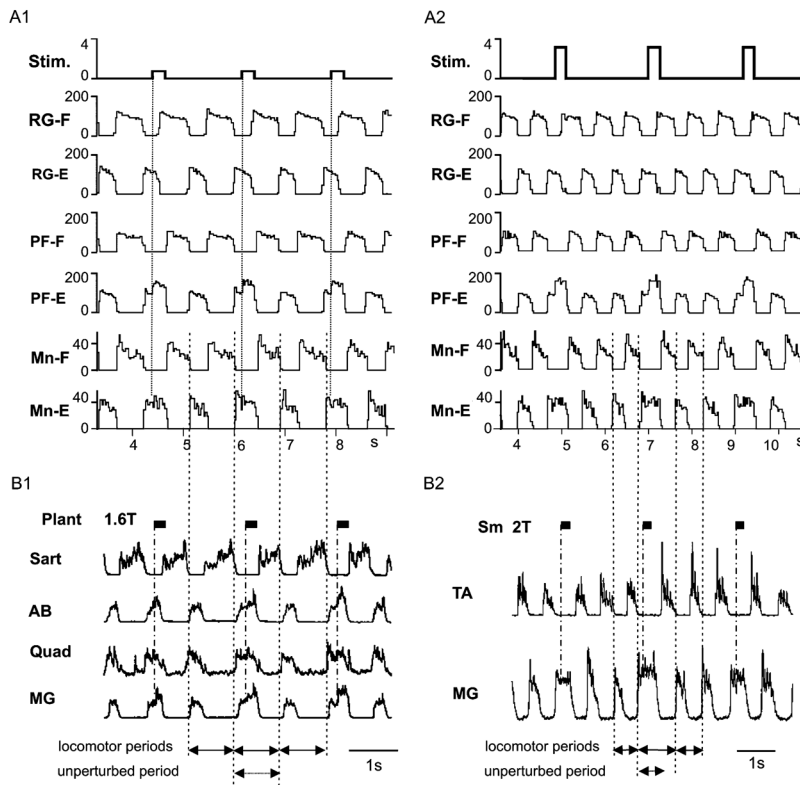
Fig. 7.
Modeling the effects of group I extensor afferent stimulation during extension. (A1 and A2) Examples of modeling the effects of stimulation of group I extensor afferents during extension (see text for details). The applied stimuli are shown in the top traces. The stimulus amplitude in A2 was three times than in A1. (B1 and B2) The effects of stimulation of extensor group I afferents during MLR-evoked fictive locomotion. In panel B1, stimulation of plantaris (Plant) group I afferents during extension increased the size and duration of extensor motoneuron activity (MG) and shortened the duration of the following flexor phase as seen in the sartorius (Sart) ENG. Note that in both A1 and B1, the duration of each flexion phase following the prolonged extension phase was shortened so that the locomotor periods did not change. The locomotor rhythm was not reset (see equal length arrows at the bottom). In panel B2, hip extensor (Sm) muscle afferents were electrically stimulated during extension. In contrast to A1 and B1, in both A2 and B2 the flexion phase that follows the stimulus-evoked extension phase prolongation was not shortened and the step cycle period increased with each stimulus delivery (see arrows at the bottom). Adapted with permission from Rybak et al. (2006b).